

Dynamics of a nonlinear parametrically excited partial differential equation

W. I. Newman

*Departments of Earth and Space Sciences, Physics and Astronomy, and Mathematics,
University of California, Los Angeles, California 90095*

R. H. Rand

Department of Theoretical and Applied Mechanics, Cornell University, Ithaca, New York 14853

A. L. Newman

Department of Physics, California State University at Dominguez Hills, Carson, California 90747

(Received 17 August 1998; accepted for publication 18 November 1998)

We investigate a parametrically excited nonlinear Mathieu equation with damping and limited spatial dependence, using both perturbation theory and numerical integration. The perturbation results predict that, for parameters which lie near the 2:1 resonance tongue of instability corresponding to a single mode of shape $\cos nx$, the resonant mode achieves a stable periodic motion, while all the other modes are predicted to decay to zero. By numerically integrating the p.d.e. as well as a 3-mode o.d.e. truncation, the predictions of perturbation theory are shown to represent an oversimplified picture of the dynamics. In particular it is shown that steady states exist which involve many modes. The dependence of steady state behavior on parameter values and initial conditions is investigated numerically. © 1999 American Institute of Physics. [S1054-1500(99)00601-1]

We consider a large (or infinite degree of freedom) nonlinear problem, with its origin in laboratory experiments, that constitutes the physical realization of an ideal situation usually described by the sine-Gordon equation and the formation of a soliton. Owing to the presence of physical dissipation, we must introduce energy into the problem to compensate for frictional losses, and this alters the character of the underlying problem, rendering it nonintegrable. Nevertheless, the observed behavior appears to be very simple, describable by a very low degree of freedom system. The mechanical driver employed to sustain the problem introduces the potential for parametric resonance, and this in turn produces a form of stable periodic motion analogous to (yet very different from) that predicted by sine-Gordon theory. We develop a low-order truncated mode perturbation theory for this problem, and compare its predictions with very accurate simulations of the underlying laboratory experiment. We perform extensive numerical experiments to identify departures of the theory from experiment. While the perturbation theory is often useful, we observe in some situations that perturbation theory provides an oversimplified picture of the true dynamics.

$$\frac{\partial u}{\partial x} = 0 \quad \text{at } x=0 \quad \text{and } x=\pi. \quad (1.2)$$

Our study is motivated by two experiments performed by Bruce C. Denardo which were part of his dissertation at UCLA,^{1,2} completed in 1990 and which motivated subsequent investigations:³⁻⁷ (i) a line of coupled pendula with vertical forcing, and (ii) surface waves in a vertically forced channel of water. Equations (1.1) and (1.2) represent an approximate continuum model of the pendulum lattice, and also exhibit behavior similar to the surface wave system. Coherent localized structures were observed which led the experimenters to interpret these as being the physical realization of solitons. However, the formal definition of a soliton⁸⁻¹² requires that the underlying equation is integrable, i.e., contains an infinite number of conservation laws. The formal lack of integrability, due to the dissipation and forcing, suggested to us that an explanation might be rooted in the nonlinear dynamical interaction of modes. The purpose of the present paper is to compare a truncated-mode perturbation treatment of these equations (valid for small ϵ), with a direct numerical integration of the p.d.e. The predictions of the model were in qualitative agreement with the experimental results reported above.

The experimenters observed the formation of coherent localized structures in a situation similar to one described by the sine-Gordon⁸ equation. The sine-Gordon equation supports soliton behavior⁹ and is integrable^{10,11} via the Backlund transformation and the inverse scattering transformation.¹² Since the wave amplitudes were small, the sinusoidal term could be approximated by a cubic expansion. However, as the physical environment was dissipative, it was essential that the experiment contain a forcing mechanism so that the system could develop some kind of stationary behavior. With

I. INTRODUCTION

This work concerns the dynamical behavior of the following partial differential equation,

$$\frac{\partial^2 u}{\partial t^2} - c^2 \frac{\partial^2 u}{\partial x^2} + \epsilon \beta \frac{\partial u}{\partial t} + [\delta + \epsilon \gamma \cos t]u = \epsilon \alpha u^3 \quad (1.1)$$

with the boundary conditions

the simplification of the sine term to a cubic expansion and, especially, with the introduction of a physical damping and forcing term, the formal integrability properties of the equation were eliminated. Owing to the truncation of the sine term in our problem, we also have lost the periodicity implicit to the sine-Gordon problem. Thus, we might expect to see behavior in our problem that is more symptomatic of the nonlinear Schrödinger equation due to this symmetry breaking. Nevertheless, the experimental system did exhibit some localized coherent-structures or nonlinear standing waves, depending upon the starting conditions and the degree of damping and forcing present.

Bishop *et al.*^{13,14} have considered a closely related problem (where the sine was not approximated by a cubic polynomial) in the context of how chaotic properties might manifest. Ercolani *et al.*¹⁵ employed the integrability properties of the sine-Gordon equation in developing a variation of parameters approach to modal expansions. Unlike these other papers, the physical system we have selected is susceptible to parametric resonance effects. P.D.E. methods were employed¹⁶ to explore a problem related to the one at hand, in the sense that they too were concerned with the effects of parametric excitation. A Karhunen-Loève expansion was employed to identify the dominant modes in the simulated p.d.e. evolution, as well as other soliton-related methods. In contrast with these earlier works—investigations that were predicated upon p.d.e. and soliton theory—our approach is to explore our problem by means of o.d.e. methods and the truncation of a natural basis set as well as to explore the hypothesis that there exists an attractor for this system consisting of only a few modes.

We are particularly interested in the latter physical manifestation of the experiments—the emergence of nonlinear standing waves. Although visually complex, the observations appeared to be describable by a small set of spatially interacting modes, coupled only through the nonlinearity in (1.1). It is this hypothesis, which allows us to approximate the partial differential equation (1.1) by a set of ordinary differential equations, that is the subject of this paper.

Equation (1.1) may be thought of as a generalization of the Mathieu equation,

$$\frac{d^2u}{dt^2} + [\delta + \epsilon \cos t]u = 0 \tag{1.3}$$

to which nonlinear ($\epsilon\alpha u^3$) and damping ($\epsilon\beta du/dt$) terms, as well as spatially-dependent ($c^2 \partial^2 u / \partial x^2$) terms have been added. Equation (1.3) has been studied by many authors. For example, Stoker¹⁷ presents a perturbation approach valid for small ϵ to discuss the dynamics of Eq. (1.3) in the neighborhood of 2:1 resonance, $\delta = 1/4 + O(\epsilon)$, i.e., when the forcing frequency ($=1$) is nearly twice the natural frequency ($=\sqrt{\delta} \approx 1/2$). The well-known result is that the rest solution $u \equiv 0$ is unstable for

$$\left| \delta - \frac{1}{4} \right| \leq \frac{\epsilon}{2} + O(\epsilon^2) \tag{1.4}$$

and stable for all other parameters near the 2:1 resonance (see Fig. 1).

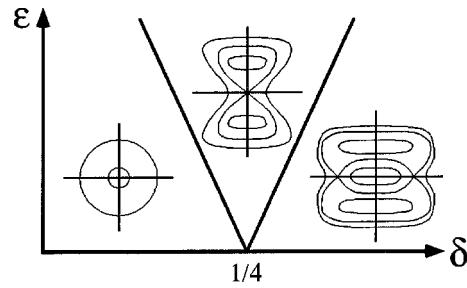


FIG. 1. Tongue of instability (1.4) for Eqs. (1.3) and (1.5) for parameters near the 2:1 resonance at $\delta = 1/4$, $\epsilon = 0$. Displayed are schematic representations of typical Poincaré maps in the $u-u'$ plane for Eq. (1.5) as obtained by perturbation theory.

A version of Eq. (1.1) in which spatially-dependent and damping terms have been omitted has been previously studied by Nayfeh and Mook,¹⁸ Holmes and Rand,¹⁹ and Month and Rand,²⁰ namely,

$$\frac{d^2u}{dt^2} + [\delta + \epsilon \cos t]u = \epsilon\alpha u^3. \tag{1.5}$$

These authors used perturbation methods valid for small ϵ and restricted to a neighborhood of 2:1 resonance, $\delta = 1/4 + O(\epsilon)$, to discuss the effect of the nonlinear term $\epsilon\alpha u^3$ on Mathieu's Eq. (1.3). It was found that for $\alpha > 0$, $0 < \epsilon \leq 1$, there are 0, 1, or 2 periodic solutions in addition to the trivial solution $u \equiv 0$, depending on the values of δ and ϵ ;

$$\begin{aligned} \delta - \frac{1}{4} &\leq -\frac{\epsilon}{2} && 0 \text{ periodic solutions} \\ -\frac{\epsilon}{2} < \delta - \frac{1}{4} < \frac{\epsilon}{2} && 1 \text{ periodic solution (stable)} \\ \frac{\epsilon}{2} &\leq \delta - \frac{1}{4} && 2 \text{ periodic solutions} \\ &&& (1 \text{ stable, 1 unstable}). \end{aligned} \tag{1.6}$$

See Fig. 1, where the Poincaré map associated with a surface of section $\Sigma: t = 0 \pmod{2\pi}$ is displayed for each of these three cases. The effect of the nonlinear term $\epsilon\alpha u^3$ may be described in words as follows: The region of instability in Eq. (1.4) associated with the linear Mathieu Eq. (1.3) persists, but the unbounded growth which occurs in (1.3) is replaced by a finite amplitude periodic motion. The nonlinearity gives rise to an amplitude-dependent shift in frequency of the unforced system which may be thought of as balancing the parametric resonance. The effect of including a damping term $\epsilon\beta du/dt$ is to break the saddle connections in Fig. 1, and to change the centers into sinks.

The foregoing discussion summarizes the perturbation results for the o.d.e. version of Eq. (1.1), i.e., Eq. (1.1) when $c = 0$ or when $u(x, t)$ is a function of time alone. In the rest of this paper we shall be interested in the effects of including a spatially dependent term $c^2 \partial^2 u / \partial x^2$. In the next section we develop a perturbation solution to Eq. (1.1) comparable to the perturbation approaches obtained previously for the o.d.e. version of Eq. (1.1). Then we compare the predictions

of the perturbation method with direct numerical integration of the p.d.e. (1.1) and of systems of o.d.e. truncations of (1.1).

II. PERTURBATION METHOD

In order to satisfy the boundary conditions (1.2), we assume a solution in the form of an infinite series

$$u = f_0(t) + f_1(t)\cos x + f_2(t)\cos 2x + \dots \tag{2.1}$$

Substituting (2.1) into (1.1) and simplifying the trigonometric terms in u^3 gives

$$\dot{f}_n + \omega_n^2 f_n + \epsilon(\beta \dot{f}_n + \gamma f_n \cos t) = \epsilon \alpha g_n, \tag{2.2}$$

where $\omega_n^2 = \delta + n^2 c^2$ and where g_n is a cubic in all the f_i 's. For example, the expression for g_0 obtained by using MACSYMA after truncating terms beyond f_6 is

$$g_0 = \frac{3}{2}f_0 f_6^2 + \frac{3}{2}f_1 f_5 f_6 + \frac{3}{2}f_2 f_4 f_6 + \frac{3}{4}f_3^2 f_6 + \frac{3}{2}f_0 f_5^2 + \frac{3}{2}f_1 f_4 f_5 + \frac{3}{2}f_2 f_3 f_5 + \frac{3}{2}f_0 f_4^2 + \frac{3}{2}f_1 f_3 f_4 + \frac{3}{4}f_2^2 f_4 + \frac{3}{2}f_0 f_3^2 + \frac{3}{2}f_1 f_2 f_3 + \frac{3}{2}f_0 f_2^2 + \frac{3}{4}f_1^2 f_2 + \frac{3}{2}f_0 f_1^2 + f_0^3 + \dots$$

For convenience in what follows, we write (2.2) in the abbreviated form

$$\dot{f}_n + \omega_n^2 f_n = \epsilon Q_n, \tag{2.3}$$

where $Q_n = -\beta \dot{f}_n - \gamma f_n \cos t + \alpha g_n$.

When $\epsilon = 0$, the solution to (2.3) may be written

$$f_n = R_n \cos(\omega_n t + \psi_n), \tag{2.4}$$

where R_n and ψ_n are constants. When $\epsilon > 0$, we look for a solution to (2.3) in the form (2.4) with R_n and ψ_n as functions of t (variation of parameters).

As we show in Appendix A, R_n and ψ_n satisfy the differential equations

$$\dot{R}_n = -\epsilon \frac{Q_n}{\omega_n} \sin(\omega_n t + \psi_n), \tag{2.5}$$

$$R_n \dot{\psi}_n = -\epsilon \frac{Q_n}{\omega_n} \cos(\omega_n t + \psi_n). \tag{2.6}$$

Next we use the method of averaging to replace Eqs. (2.5) and (2.6) by simpler, though approximate equations, a procedure which is valid for small ϵ . See Appendix B for the details of the computation, which involves replacing the right-hand sides of (2.5) and (2.6) with their average values (averaged in t , holding R_n and ψ_n fixed).

For general (nonresonant) values of the parameters, Eq. (2.5) on R_n averages to

$$\dot{R}_n = -\epsilon \frac{\beta}{2} R_n. \tag{2.7}$$

All solutions to (2.7) decay to zero. We thus come to the first conclusion, namely that *unless we are in the neighborhood of a resonance* (to be discussed next), *all motions are predicted to damp out.*

If, however, $\omega_n = 1/2$, then there will be an extra term in the averaged Eq. (2.7), namely,

$$\dot{R}_n = -\epsilon \frac{\beta}{2} R_n + \epsilon \frac{\gamma}{2} R_n \sin 2\psi_n. \tag{2.8}$$

Since $\omega_n^2 = \delta + n^2 c^2$, such a resonance relation can exist for only a single value of n (for fixed values of δ and c). Thus in the case of such a resonance, all modes except the resonant mode will have averaged equations of the form (2.7), i.e., they will decay to zero.

In order to find out what happens to the resonant mode, we have to examine the averaged version of Eq. (2.6) on ψ_n . Before doing so, we generalize the discussion to allow for detuning from resonance, that is

$$\omega_n^2 = \frac{1}{4} + \Delta \epsilon, \tag{2.9}$$

where Δ is a detuning coefficient.

In computing the averaged version of Eq. (2.6) on the resonant mode ψ_n (see Appendix B), we use the fact that the amplitudes R_i of all the nonresonant modes decay to zero, and we restrict attention to the long-time behavior. In doing so we obtain simplified equations for ψ_n , which are valid after the transients associated with the decay of the nonresonant modes die out, namely,

$$\dot{\psi}_n = \epsilon \Delta + \epsilon \frac{\gamma}{2} \cos 2\psi_n - \frac{9}{16} \epsilon \alpha R_n^2, \quad n > 0, \tag{2.10}$$

$$\dot{\psi}_0 = \epsilon \Delta + \epsilon \frac{\gamma}{2} \cos 2\psi_0 - \frac{3}{4} \epsilon \alpha R_0^2, \quad n = 0. \tag{2.11}$$

III. STEADY STATE RESONANCE

The averaged equations governing resonance are Eqs. (2.8), (2.10), and (2.11). At steady state these slow flows will approach their stable equilibria, each equilibrium corresponding to a periodic motion of the original system. These will satisfy the equations,

$$\beta = \gamma \sin 2\psi_n, \tag{3.1}$$

$$\Delta + \frac{\gamma}{2} \cos 2\psi_n - \frac{9}{16} \alpha R_n^2 = 0, \quad n > 0, \tag{3.2}$$

$$\Delta + \frac{\gamma}{2} \cos 2\psi_0 - \frac{3}{4} \alpha R_0^2 = 0, \quad n = 0. \tag{3.3}$$

From (3.1) we see that $\sin 2\psi_n = \beta/\gamma$. Substituting this into (3.2) and (3.3), we obtain the steady state amplitudes

$$R_n^2 = \frac{16}{9\alpha} \left[\Delta \pm \frac{1}{2} \sqrt{\gamma^2 - \beta^2} \right], \quad n > 0, \tag{3.4}$$

$$R_0^2 = \frac{4}{3\alpha} \left[\Delta \pm \frac{1}{2} \sqrt{\gamma^2 - \beta^2} \right], \quad n = 0. \tag{3.5}$$

As an example, take the case where the damping β is zero, and where $n > 0$. Then

$$R_n^2 = \frac{16}{9\alpha} \left[\Delta \pm \frac{1}{2} \gamma \right], \quad n > 0. \tag{3.6}$$

But R_n^2 must be non-negative. As a result, there will be 0, 1, or 2 solutions (in addition to the trivial solution $R_n = 0$), depending on Δ , hence

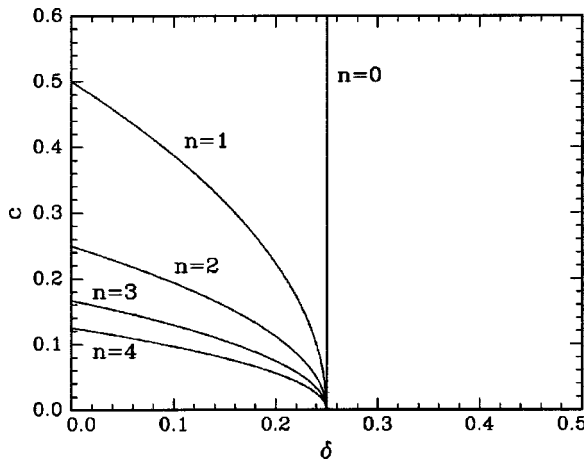


FIG. 2. The resonance curves of Eq. (3.10) for $n=0,1,2,3,4$.

$$\Delta < -\gamma/2 \rightarrow 0 \text{ periodic solutions,} \tag{3.7}$$

$$\Delta > -\gamma/2 \text{ but } \Delta < \gamma/2 \rightarrow 1 \text{ periodic solution,} \tag{3.8}$$

$$\Delta > \gamma/2 \rightarrow 2 \text{ periodic solutions.} \tag{3.9}$$

It turns out that these changes in the number of periodic solutions coincide with changes in stability of the trivial solution $R_n=0$ (as may be shown by considering the slow flow linearized near $R_n=0$). In cases (3.7) and (3.9), the trivial solution is stable, while it is unstable in the case of (3.8). In (3.8), the nontrivial periodic solution is stable, while in (3.9) one of the nontrivial periodic solutions is stable, and one is unstable. In cases (3.8) and (3.9), the stable motion corresponds to the + sign in Eqs. (3.4) and (3.5).

If there is small damping, the results are similar, except the stable equilibria of the slow flow change from centers to sinks. These stable periodic solutions are the unique asymptotic state for given values of the parameters, independent of initial conditions, except if two stable states coexist [as in (3.9), where the rest solution $u=0$ is also stable].

Now suppose that we fix the values of the parameters α, β, γ , and ϵ , and ask how the steady state dynamics of Eqs. (1.1), (1.2) change as δ and c are varied. We refer the reader to Fig. 2 which shows the resonances

$$\omega_n^2 = \delta + n^2 c^2 = \frac{1}{4} \tag{3.10}$$

for $n=0,1,2,3,4$ plotted in the δ - c plane. The perturbation analysis is valid in the neighborhood of each of these curves, and predicts that a stable periodic motion of the form

$$u(x,t) = R_n \cos(\omega_n t + \psi_n) \cos nx, \tag{3.11}$$

where R_n and ψ_n are constants [cf. Eqs. (3.4) and (3.5)], exists on these curves.

In the case of detuning, cf. Eq. (2.9), each resonance curve has a region in its neighborhood in which the rest solution $u=0$ is unstable (see Fig. 3). The boundaries of these instability regions (or Arnold tongues) are given by $\Delta = \pm \gamma/2$, cf. (3.7)–(3.9), or by

$$\delta + n^2 c^2 = \frac{1}{4} \pm \frac{\gamma}{2} \epsilon + O(\epsilon^2). \tag{3.12}$$

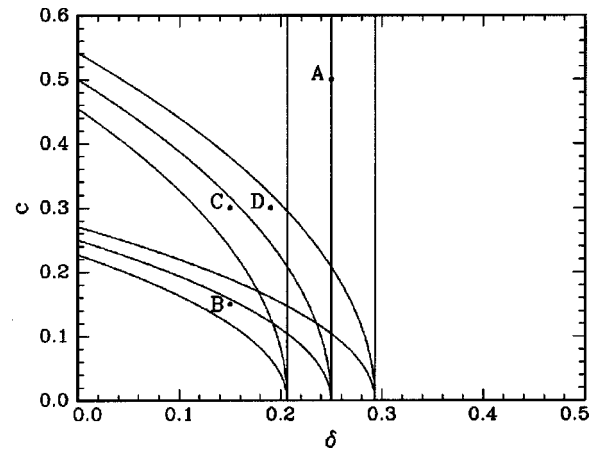


FIG. 3. The instability regions of Eq. (3.12) and the resonance curves of Eq. (3.10) for $\gamma=1, \epsilon=0.1$, and $n=0,1,2$. The points A, B, C, D refer to example systems discussed in the text.

For points inside these regions, a stable periodic motion of the form (3.11) is predicted to exist. For $\alpha > 0$, points lying outside a region (3.12), but on its right-hand side, are predicted to involve two stable states (a periodic solution of known amplitude, and the trivial solution). For points outside of (3.12) on its left-hand side, however, only the trivial solution is stable. In the case where two stable solutions exist, the question of which one occurs depends on the initial conditions.

Note that while the resonance curves (3.10) intersect only at $\delta=1/4, c=0$, the associated instability regions (3.12) overlap. At points in the overlap regions, we may expect that periodic motions of the form (3.11) exist for each of the values of n corresponding to each of the overlapping regions. In this region, multiple resonances are expected to be important.

The foregoing perturbation theory gives a charmingly simple picture of the steady state dynamics of Eqs. (1.1) and (1.2), at least for small ϵ and in the neighborhood of 2:1 resonance. The rest of this paper consists of a comparison between the perturbation theory predictions and the actual behavior of the p.d.e. (1.1) as obtained by numerical integration.

IV. NUMERICAL INTEGRATION OF THE P.D.E.

The simulation of hyperbolic p.d.e.'s is often a daunting task, particularly since their long-time evolution is marginally stable.²¹ It is essential, for our purpose, that the methodology employed introduce no significant dissipation and be capable of preserving the precise character of the solution over hundreds of oscillation periods. Consequently, we felt it would be inappropriate to use conventional second-order methodologies, i.e., those whose truncation error is $O(\Delta x^2, \Delta t^2)$. We applied methods that were at least fourth order in both space and time. The first class of methods we considered were of spectral²² or Galerkin²³ type. A natural expansion emerges from the cosine function over the interval $(0, \pi)$, i.e., $\cos nx$ for $n=0,1,\dots$, since this defines a complete basis set whose derivatives vanish at the end points. (Conceptually, this spectral or Galerkin scheme is a natural

extension of the truncated basis set that we employ in our analytic calculations. The use of this methodology also provided a quantitative confirmation of our ansatz that a low order truncated mode expansion, i.e., 3 modes, was sufficient.)

We employed a basis set with 128 terms, so that we could exploit the computational efficacy of the Fast Fourier Transform. Formally, the nonlinearities present in the spatial operator required that we employ a ‘‘pseudospectral method’’²³ to accurately and rapidly approximate the right-hand side of the partial differential equation. Pseudospectral methods convert partial differential equations into ordinary differential equations, thereby reducing their computational complexity. The resulting set of ordinary differential equations can be solved using a fourth order integration scheme. We employed a standard fourth order Runge–Kutta²⁴ for this purpose. Although this method is not computationally optimal, it is extremely simple to implement and requires no special starting procedure. Extensive testing of this procedure, particularly in the limit where we can analytically establish the exact solution, showed that it was reliable and accurate to five significant figures over hundreds of oscillation periods. However, this accuracy was obtained at the expense of computation time and the overhead associated with the repeated performance of FFT’s. To overcome the high cost of this otherwise desirable approach, we considered alternatives to our method for evaluating the spatial operator.

We selected the so-called ‘‘method of lines.’’²⁵ The basic feature of this method is that the derivatives with respect to one of the independent variables (i.e., time) remain continuous, while derivatives with respect to the other independent variables are replaced by finite-difference approximations. The method of lines is essentially a technique for replacing a system of partial differential equations by a system of ordinary differential equations, like pseudospectral methods, using local Taylor series (in contrast with Fourier series) to develop the expansion. Recently, Holt²⁶ and Schiesser²⁷ have explored this methodology. In our situation, the boundary conditions are relatively simple since, it can be shown, $u_x = u_{xxx} = 0$ at each boundary. Hence, we can define two ‘‘image’’ points on the other side of each boundary which turn out to be mirror images of the respective points inside the boundary. A five-point central difference operator can therefore be used over the entire interval to estimate the spatial operator or, equivalently, the right-hand side of the partial differential equation with an error of $O(\Delta x^2)$. Employing a computational grid for the method of lines with the same resolution as that employed in the 128 point pseudospectral expansion produced results which were identical over four significant figures over 100 oscillation periods of the system. Remarkably, however, the simplicity of the five-point finite difference operator in contrast with the FFT, provided nearly an order of magnitude improvement of the computational speed with no significant diminution of accuracy.

We generally chose our initial conditions in the form

$$u(x,0) = a_0 + a_1 \cos x + a_2 \cos 2x, \quad u_t(x,0) = 0, \quad (4.1)$$

where we specified the initial Fourier components $a_0, a_1,$ and a_2 . We numerically integrated the system (1.1) and (1.2) for 800 time units or greater, at which point steady state was approximately achieved. Then we Fourier expanded in x the numerical solution to obtain

$$u(x,t) = f_0(t) + f_1(t) \cos x + f_2(t) \cos 2x + \dots + f_{20}(t) \cos 20x, \quad (4.2)$$

where $f_n(t)$ is the Fourier component with wave number n .

In order to restrict the complexity of the problem, all of the numerical experiments which we report here correspond to the parameter values

$$\alpha = 1, \quad \beta = \frac{1}{2}, \quad \gamma = 1, \quad \epsilon = 0.1. \quad (4.3)$$

For these fixed parameter values, we vary δ and c as well as the initial conditions (4.1).

A comparison of the predictions of the perturbation approach with the results of numerical integration may be illustrated with some examples. We present results for four typical points labeled A, B, C, D in Fig. 3. In each case initial conditions (4.1) are taken in the form

$$u(x,0) = 0.1 + 0.1 \cos x + 0.1 \cos 2x, \quad u_t(x,0) = 0. \quad (4.4)$$

For point $A: (\delta, c) = (0.25, 0.5)$, numerical integration produced a periodic motion with all $f_n(t) \equiv 0$ except $f_0(t)$, which had amplitude 0.77. To compare this result with perturbation theory, we note that since $\delta = 0.25$, the detuning Δ of $\omega_0^2 = \delta = 0.25$ in Eq. (2.9) is zero, so that the predicted amplitude R_0 of the $n = 0$ mode in Eq. (3.5) is given by $R_0 = 0.76$.

For point $B: (\delta, c) = (0.15, 0.15)$, numerical integration produced a periodic motion with all $f_n(t) \equiv 0$ except $f_2(t)$, which had amplitude 0.78. This time the detuning of $\omega_2^2 = \delta + 4c^2 = 0.24$ is given by $\Delta = -0.1$, yielding predicted amplitude $R_2 = 0.77$ in Eq. (3.4).

For point $C: (\delta, c) = (0.15, 0.3)$, numerical integration produced a periodic motion with all even modes $f_{2n}(t) \equiv 0$, while $f_1(t)$ had amplitude 0.78, $f_3(t)$ had amplitude 0.01 and the other odd modes had amplitude ≤ 0.001 . This time the detuning of $\omega_1^2 = \delta + c^2 = 0.24$ is given by $\Delta = -0.1$, yielding predicted amplitude $R_1 = 0.77$ in Eq. (3.4).

Thus there is excellent agreement between perturbation theory and numerical integration for points $A, B,$ and C . Not so for point D , however.

For point $D: (\delta, c) = (0.19, 0.3)$, numerical integration produced a quasiperiodic motion with all modes present (see Fig. 4). The approximate amplitudes of $f_0(t), f_1(t), f_2(t)$ are, respectively, given by 0.3, 0.9, 0.3, although these values vary slightly from cycle to cycle since the motion is not periodic. The corresponding amplitudes of the higher modes are $\text{all} \leq 0.03$. We shall refer to this steady state as a multi-mode response. The frequencies of the modes $n = 0, 1, 2$ (which also vary from cycle to cycle) are approximately found to be $\omega_0 = 0.33, \omega_1 = 0.5, \omega_2 = 0.67$, and hence represent a resonance in the ratio

$$\omega_0 : \omega_1 : \omega_2 : \omega_d :: 2 : 3 : 4 : 6, \quad (4.5)$$

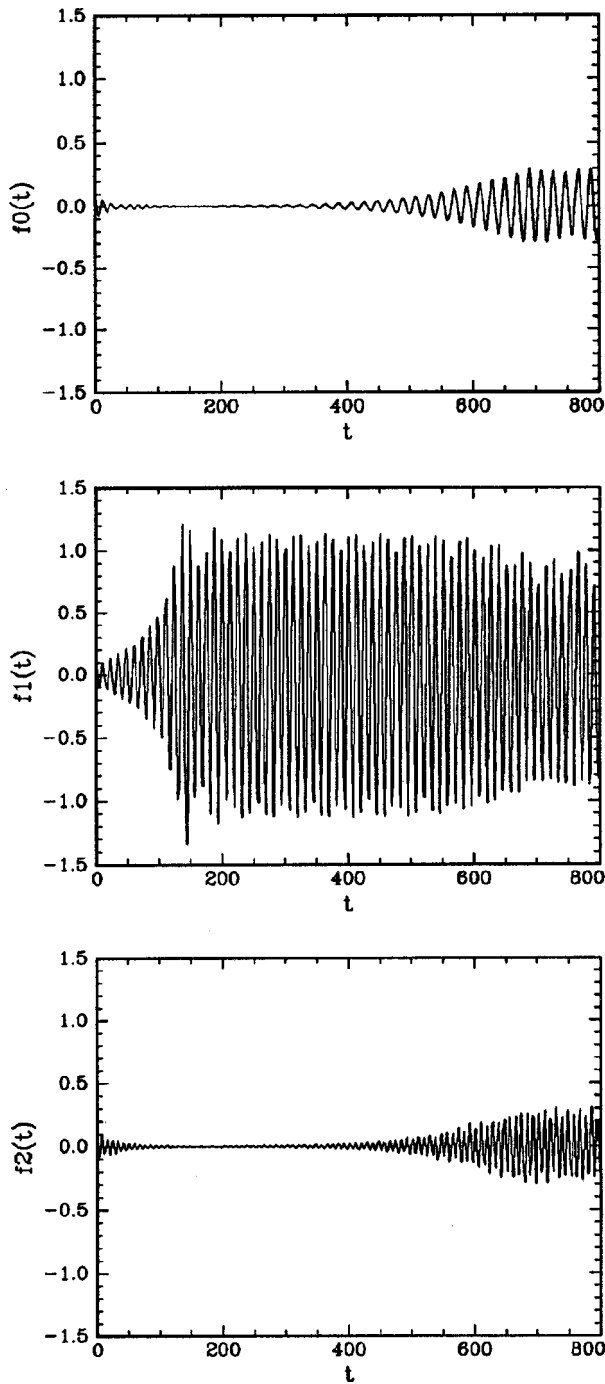


FIG. 4. Numerical integration of the p.d.e. (1.1) and (1.2). The functions $f_n(t)$ are the Fourier components of Eq. (4.2). Parameters correspond to point D in Fig. 3, cf. Eqs. (4.3), (4.4). Note the multimode behavior of the steady state.

where $\omega_d=1$ is the frequency of the driver $\cos t$. In this case the perturbation result is completely wrong; the detuning of $\omega_1^2 = \delta + c^2 = 0.28$ is given by $\Delta = 0.3$, yielding the predicted amplitude of a lone periodic $n=1$ mode of $R_1 = 1.14$ in Eq. (3.4). No such lone $n=1$ mode is observed.

Another feature which is present in the dynamics of the p.d.e., but which is missing from the perturbation theory, is the possibility of unbounded growth. The presence of the

nonlinearity in the form $\epsilon \alpha u^3$ is responsible for this phenomenon, in contrast to a more realistic nonlinearity of the form $\sin u$. The absence of unbounded growth from the perturbation theory may be due to the scaling by small ϵ , which localizes the dynamics around the origin $u \equiv 0$.

V. THREE-MODE TRUNCATION

Another feature observed in our numerical experiments is that, generally speaking, the steady state is dependent on the initial conditions. This phenomenon is well known in

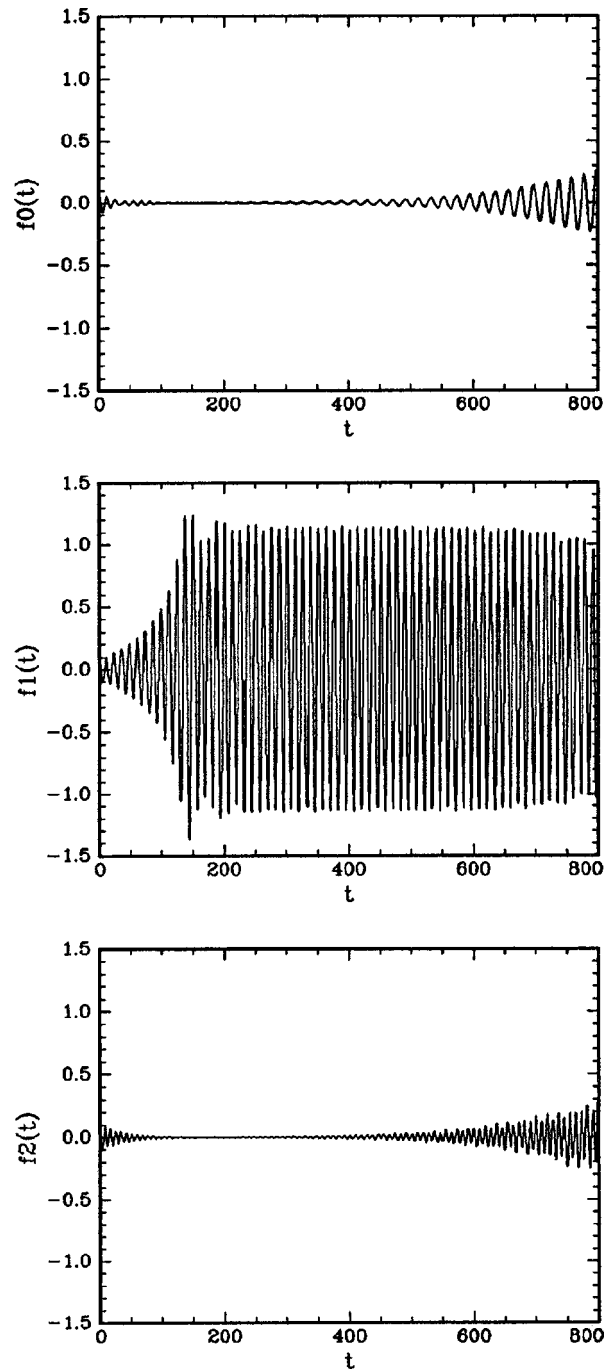


FIG. 5. Numerical integration of the three-mode o.d.e. truncation (5.1)–(5.3). Parameters and initial conditions are the same as for Fig. 4.

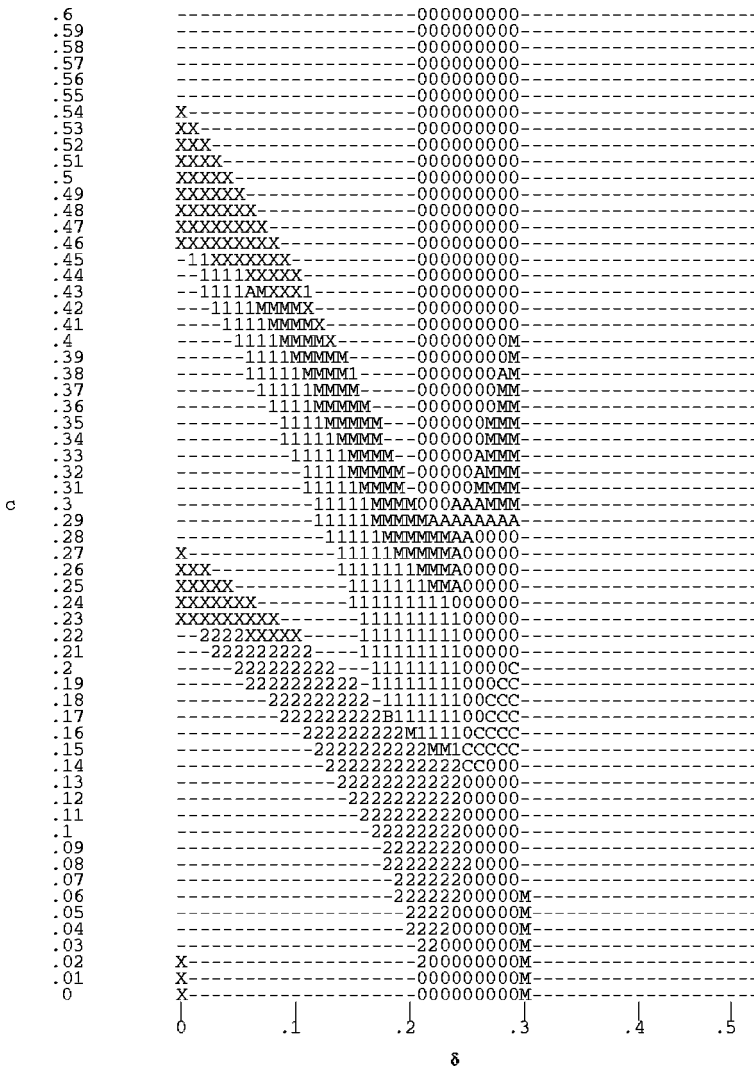


FIG. 6. Results of numerical integration of the three-mode o.d.e. truncation for parameters (4.3), for initial conditions $(f_0(0)=0.1, f_1(0)=0.1, f_2(0)=0.1)$, and for zero initial velocities. See (5.4) for the meaning of symbols.

finite dimensional problems, i.e., in systems of o.d.e.'s. A familiar example is a 2π -periodically forced single degree of freedom oscillator, where the dependency of steady state on initial conditions may be displayed by giving the boundaries of the basins of attraction on a Poincaré section with cut at $t=0 \pmod{2\pi}$ (see Ref. 28, for example). The present situation is much more complicated, however, because of the infinite dimensional nature of the dynamics, i.e., we may think of the p.d.e. (1.1) as a system of an infinite number of coupled oscillators, each corresponding to a single mode cnx .

In order to investigate the dependency of steady state on initial conditions in an efficient manner, we consider a three mode o.d.e. truncation of the infinite system (2.2),

$$\begin{aligned} \dot{f}_0 + \omega_0^2 f_0 + \epsilon(\beta \dot{f}_0 + \gamma f_0 \cos t) \\ = \epsilon \alpha [3f_0^3 + \frac{3}{2}f_0 f_2^2 + \frac{3}{4}f_1^2 f_2 + \frac{3}{2}f_0 f_1^2], \end{aligned} \tag{5.1}$$

$$\begin{aligned} \dot{f}_1 + \omega_1^2 f_1 + \epsilon(\beta \dot{f}_1 + \gamma f_1 \cos t) \\ = \epsilon \alpha [3f_0^2 f_1 + \frac{3}{4}f_1^3 + \frac{3}{2}f_1 f_2^2 + 3f_0 f_1 f_2], \end{aligned} \tag{5.2}$$

$$\begin{aligned} \dot{f}_2 + \omega_2^2 f_2 + \epsilon(\beta \dot{f}_2 + \gamma f_2 \cos t) \\ = \epsilon \alpha [3f_0^2 f_2 + \frac{3}{4}f_2^3 + \frac{3}{2}f_1^2 f_2 + \frac{3}{2}f_0 f_1^2], \end{aligned} \tag{5.3}$$

where $\omega_0^2 = \delta$, $\omega_1^2 = \delta + c^2$ and $\omega_2^2 = \delta + 4c^2$.

Here we have selected 3 modes (rather than 2 or 4, say) because the multimode response (4.5) observed in the p.d.e. chiefly involved 3 modes.

Numerical simulation of the truncated system (5.1)–(5.3) by a fourth-order Runge–Kutta has shown that it gives a good approximation of the p.d.e. (1.1) and (1.2) for some parameters and for initial conditions of the form (4.1). For example, see Fig. 5, which shows that the 3-mode truncation exhibits the multimode behavior of Fig. 4.

We numerically integrated Eqs. (5.1)–(5.3) for a wide range of parameter values, and for each of four sets of initial conditions $(f_0(0), f_1(0), f_2(0)) = (0.1, 0.1, 0.1)$, $(1.0, 0.1, 0.1)$, $(0.1, 1.0, 0.1)$, $(0.1, 0.1, 1.0)$, the results of which are respectively displayed in Figs. 6, 7, 8, 9. All four of these figures use the following symbols to denote the observed steady state:

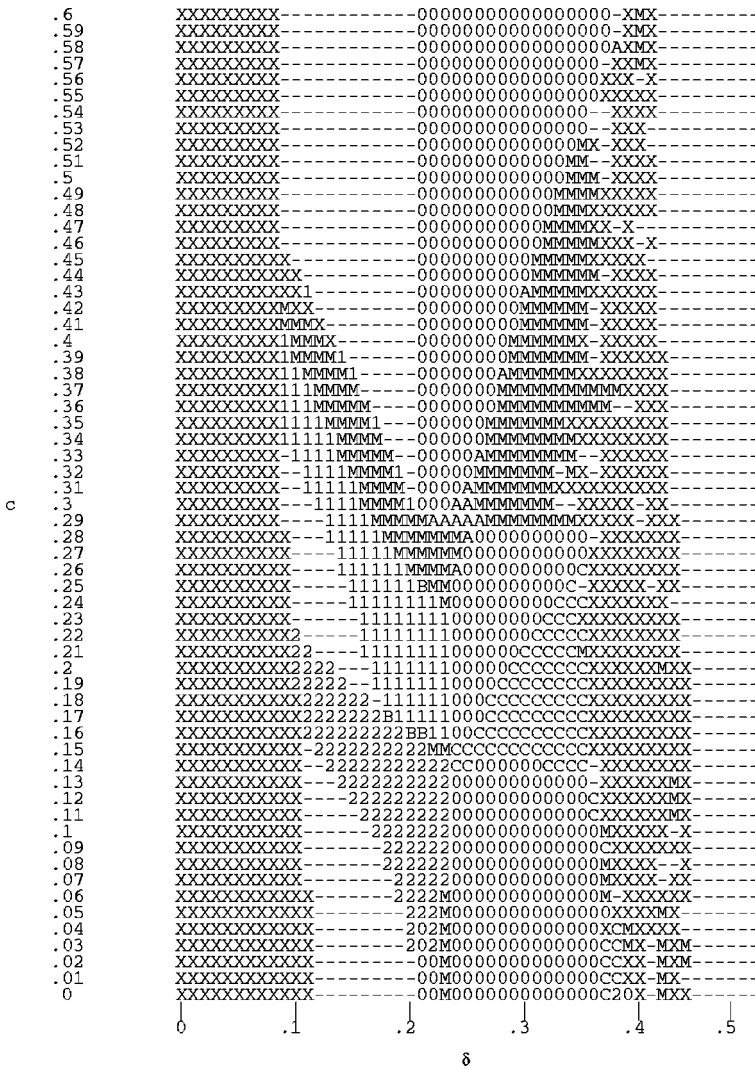


FIG. 7. Results of numerical integration of the three-mode o.d.e. truncation for parameters (4.3), for initial conditions $(f_0(0)=1.0, f_1(0)=0.1, f_2(0)=0.1)$, and for zero initial velocities. See (5.4) for the meaning of symbols.

- 0: f_0 only, $f_1=f_2=0$,
 - 1: f_1 only, $f_0=f_2=0$,
 - 2: f_2 only, $f_0=f_1=0$,
 - : trivial solution, $f_0=f_1=f_2=0$,
 - X: unbounded growth,
 - A: f_0 and f_1 only, $f_2=0$,
 - B: f_1 and f_2 only, $f_0=0$,
 - C: f_0 and f_2 only, $f_1=0$,
 - M: f_0, f_1 and f_2 all present (multimode).
- (5.4)

In all cases the initial velocities were taken as zero for simplicity. We note that in addition to the trivial motion and to the pure modes predicted by perturbation theory, a variety of mixed modes are observed, as well as unbounded growth. Comparison of these four figures shows that the dynamics of the truncated system (5.1)–(5.3) is very complicated, far more complicated than the simple picture coming from the perturbation theory presented above. Although the dynamics of the truncated system is surely not exactly the same as the

dynamics of the p.d.e. (1.1) and (1.2), it gives us an indication of the great complexity of the steady state structure of the p.d.e.

VI. DISCUSSION AND CONCLUSIONS

Inspection of Fig. 6, which corresponds to initial conditions which lie relatively close to the origin, clearly shows the regions of instability predicted by perturbation theory, cf. Fig. 3. Parameter values which lie outside these instability regions are seen to correspond to the trivial steady state (displayed as the symbol “-”), in agreement with perturbation theory. Parameter values which lie inside the instability regions are predicted by perturbation theory to lead to a lone periodic resonant mode (displayed by one of the symbols “0,” “1” or “2”). Although this prediction is fulfilled in Fig. 6 for some points inside the instability regions, there are also observed a number of multimode steady states (displayed by one of the symbols “A,” “B,” “C” or “M”). In addition, some motions are observed to lead to unbounded growth (displayed by the symbol “X”).

In contrast to Fig. 6, Figs. 7, 8, and 9 correspond to a

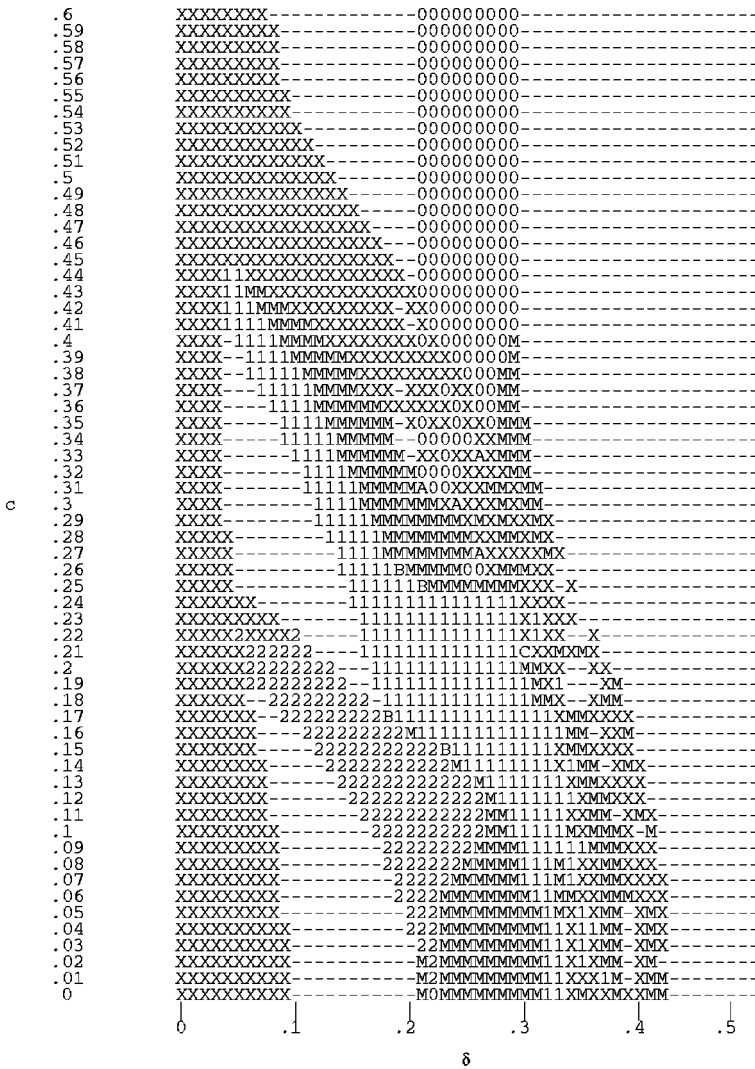


FIG. 8. Results of numerical integration of the three-mode o.d.e. truncation for parameters (4.3), for initial conditions $(f_0(0)=0.1, f_1(0)=1.0, f_2(0)=0.1)$, and for zero initial velocities. See (5.4) for the meaning of symbols.

relatively large initial condition in one of the modal amplitudes (respectively f_0, f_1, f_2), while the other two initial conditions remain small. The resulting figures have less in common with the predictions of perturbation theory than that exhibited by Fig. 6. At parameters lying outside of the regions of instability predicted by perturbation theory, the larger initial conditions of Figs. 7–9 have led to steady states other than the trivial solution. In addition, unbounded growth is seen to occur for a wider range of parameter values. Note that in each of Figs. 7, 8, and 9, the mode which is given the larger initial condition (respectively 0, 1, and 2) occurs more plentifully than in Fig. 6, especially to the right of the associated region of instability predicted by perturbation theory. This is to be expected since such an initial condition is likely to lie in the interior of the basin of attraction of the respective steady state. Note also that the steady states which involve only two components (symbolized by “A,” “B” and “C”) often lie near the boundaries of the tongues associated with their respective components. Evidently, these are multiple stable basins of attraction, in some cases corresponding both to single modes and to multiple modes. One could argue that these observations offer some support for the notion of “mode suppression.”

In this paper we have compared the predictions of a

perturbation analysis of a parametrically excited p.d.e. with numerical integration of the p.d.e. and of a three-term o.d.e. truncation. The relationship between the all too simple picture presented by the perturbation method and the extremely complicated behavior of the p.d.e. is itself complicated. The tongues of instability predicted by the perturbation theory are present in the numerically observed dynamics, but we have observed multimode steady states which are absent from the present perturbation results. These multimodes were also observed in a related two mode o.d.e. truncation.²⁹

In the perturbation scheme presented in this work, we have taken account of the possibility of a single 2:1 resonance between the driver $\cos t$ and one of the modes $f_n \cos nt$ of Eq. (2.1). The appearance of the multimodes in the numerical simulations, absent from the perturbation predictions, are conjectured to be due to multiple resonances. This has been showing in a limited way in a 2-mode analytical study²⁹ in which both the $n=0$ and $n=1$ modes are close to being in 2:1 resonance with the driver $\cos t$. The resulting dynamical behavior is shown to include stable 2-model multimodes in addition to the single-mode steady states, obtained in the present work.

The three-term o.d.e. truncation shares some of the complexity of the p.d.e. We may view the truncated approxima-

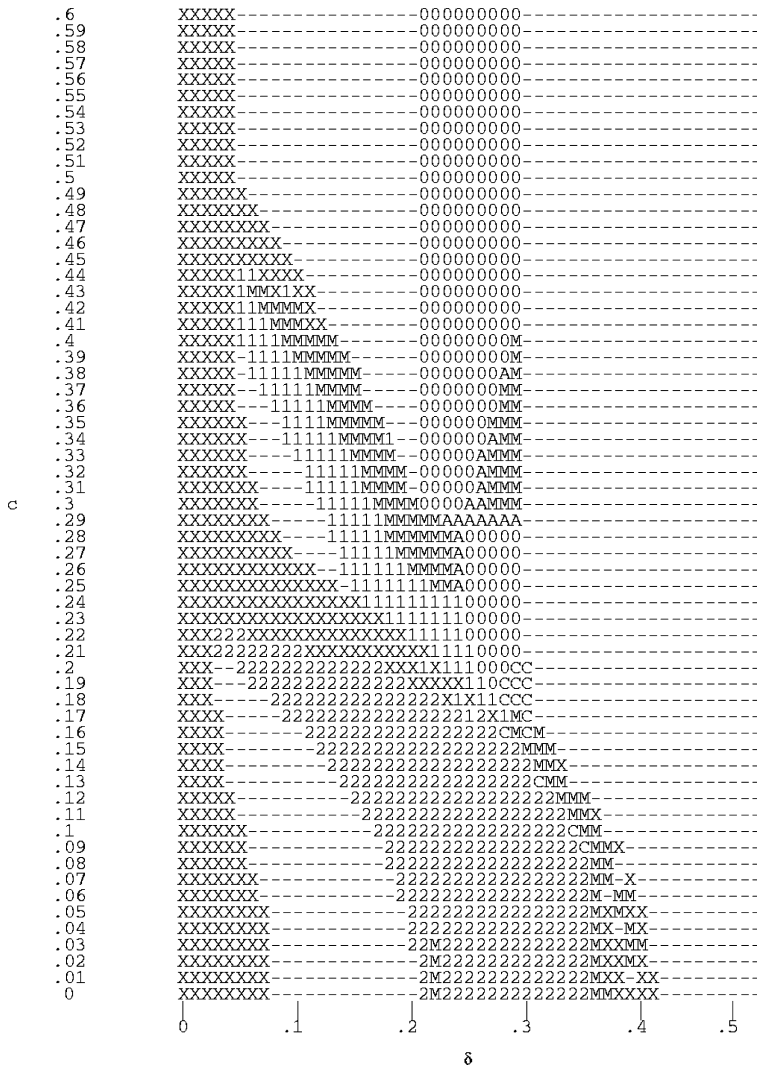


FIG. 9. Results of numerical integration of the three-mode o.d.e. truncation for parameters (4.3), for initial conditions $(f_0(0)=0.1, f_1(0)=0.1, f_2(0)=1.0)$, and for zero initial velocities. See (5.4) for the meaning of symbols.

tion as an autonomous system of four coupled o.d.e.'s (by associating the $\cos t$ forcing term with the output of a simple harmonic oscillator). Although we know of no general study of four coupled oscillators, Baesens, Guckenheimer, Kim, and MacKay³⁰ have shown that the dynamics of three coupled oscillators is extremely complicated.

We view the present paper as a first step in understanding the behavior of the p.d.e. (1.1) and (1.2). We expect additional work to be done on this system because it has numerous applications and it is a natural extension of Mathieu's equation (1.3), and thus represents a paradigm system for parametrically excited p.d.e.'s. In particular we hope for a perturbation analysis which yields the nature and bifurcation of the multimode steady states which we have observed numerically.

ACKNOWLEDGMENTS

A preliminary version of this paper appeared as an ASME conference paper.³¹ We wish to thank J.M. Hyman, D. Holm, B.C. Denardo, G. Forest, and S. Putterman for some useful discussions.

APPENDIX A: DERIVATION OF (2.5) AND (2.6)

In this appendix we derive Eqs. (2.5) and (2.6) on R_n and ψ_n . We begin by differentiating (2.4), and using the abbreviations $s = \sin(\omega_n t + \psi_n)$, $c = \cos(\omega_n t + \psi_n)$,

$$\dot{f}_n = -\omega_n R_n s + \dot{R}_n c - R_n \dot{\psi}_n s. \tag{A1}$$

As usual in the variation of parameters method, we take

$$\dot{R}_n c - R_n \dot{\psi}_n s = 0 \tag{A2}$$

so that (A1) becomes

$$\dot{f}_n = -\omega_n R_n s. \tag{A3}$$

Differentiating (A3), we find

$$\ddot{f}_n = -\omega_n^2 R_n c - \omega_n \dot{R}_n s - \omega_n R_n \dot{\psi}_n c. \tag{A4}$$

Substituting (A4) into (8), we obtain

$$-\omega_n \dot{R}_n s - \omega_n R_n \dot{\psi}_n c = \epsilon Q_n. \tag{A5}$$

Now we solve (A2) and (A5) simultaneously to get the desired Eqs. (2.5) and (2.6) of the text.

APPENDIX B: DERIVATION OF (2.7)–(2.11)

In this appendix we derive the averaged equations on R_n and ψ_n , Eqs. (2.7)–(2.11). We replace the right-hand sides of (2.5) and (2.6) with their average values (averaged in t , holding R_n and ψ_n fixed). This process may be legitimized by using a near-identity transformation, but the result to $O(\epsilon)$ is the same, so we take the simpler path.

Note from (2.3) that Q_n consists of three terms, namely,

$$Q_n = -\beta \dot{f}_n - \gamma f_n \cos t + \alpha g_n. \quad (\text{B1})$$

Note also that R_n determines the amplitude of the n th mode, while ψ_n determines its phase. We consider Eq. (2.5) first. The damping term $-\beta \dot{f}_n$ contributes to Eq. (2.5) the quantity

$$-\frac{\epsilon}{\omega_n} (-\beta) [-R_n \omega_n \sin(\omega_n t + \psi_n)] \sin(\omega_n t + \psi_n), \quad (\text{B2})$$

where we have used Eq. (A3). Equation (B2) averages to

$$-\epsilon \frac{\beta}{2} R_n. \quad (\text{B3})$$

Next consider the contribution to (2.5) from the nonlinear term αg_n . This looks like it will be difficult to compute, since g_n itself is an infinite series. However, it can be done easily, since all the terms in g_n are cubic in the f_i 's, i.e., are cubic in $\cos(\omega_i t + \psi_i)$ for all possible choices of i . Using trigonometric identities, each of these cubic terms gives a single cosine term of the form $\cos[(\omega_i \pm \omega_j \pm \omega_k)t + \psi_i \pm \psi_j \pm \psi_k]$, where i, j, k can take on any integer values. The contribution of each such term to Eq. (2.5) involves multiplying by $\sin(\omega_n t + \psi_n)$, which gives terms of the form $\sin[(\omega_i \pm \omega_j \pm \omega_k \pm \omega_n)t + \psi_i \pm \psi_j \pm \psi_k \pm \psi_n]$. Each such term has average value zero, no matter what i, j, k, n are involved. Thus the αg_n term makes no contribution to averaged equation on \dot{R}_n .

Next we consider the contribution to (2.5) coming from the term $-\gamma f_n \cos t$. This term involves the trigonometric terms $\cos(\omega_n t + \psi_n) \cos t$. When inserted into the right-hand side of Eq. (2.5), these terms get multiplied by $\sin(\omega_n t + \psi_n)$, giving terms which may be trigonometrically simplified to $\sin[(2\omega_n \pm 1)t + 2\psi_n]$. For general (nonresonant) values of the parameters, these terms have average value zero, and so make no contribution to the averaged Eq. on \dot{R}_n , which becomes

$$\dot{R}_n = -\epsilon \frac{\beta}{2} R_n. \quad (\text{B4})$$

The foregoing equation is no longer valid if the term $\sin[(2\omega_n \pm 1)t + 2\psi_n]$, just discussed, does not average to zero. Such will be the case if $\omega_n = 1/2$, for then

$$\sin[(2\omega_n - 1)t + 2\psi_n] = \sin(2\psi_n) \quad (\text{B5})$$

which behaves like a constant under averaging. In such a case, there will be an extra term in the averaged Eq. (2.7), namely

$$\dot{R}_n = -\epsilon \frac{\beta}{2} R_n + \epsilon \frac{\gamma}{2} R_n \sin 2\psi_n. \quad (\text{B6})$$

In order to find out what happens to the resonant mode, we have to examine the averaged version of Eq. (2.6) on ψ_n . Before doing so, we generalize the discussion to allow for detuning from resonance, hence,

$$\omega_n^2 = \frac{1}{4} + \Delta \epsilon, \quad (\text{B7})$$

where Δ is a detuning coefficient. From Eq. (2.2), this adds an additional term to Q_n , namely,

$$Q_n = -\beta \dot{f}_n - \gamma f_n \cos t + \alpha g_n - \Delta f_n. \quad (\text{B8})$$

Note that the additional term, $-\Delta f_n$, adds a term proportional to $\cos(\omega_n t + \psi_n) \times \sin(\omega_n t + \psi_n)$ to the right-hand side of (2.5), which averages to zero since it is proportional to $\sin(2\omega_n t + 2\psi_n)$. So the resonant mode is still governed by Eq. (2.8) in the presence of detuning.

Now we are interested in finding the averaged version of Eq. (2.6) for the resonant mode. We neglect terms of $O(\epsilon^2)$, so the factor $1/\omega_n$ becomes simply 2. We consider each of the terms in Q_n separately. First, note that the damping term $-\beta \dot{f}_n$ averages to zero. Next, note that the detuning term $-\Delta f_n$ produces the averaged contribution $\epsilon \Delta R_n$.

Next consider the contribution due to the forcing term $-\gamma f_n \cos t$. This term involves the trigonometric terms $\cos(t) \cos(\omega_n t + \psi_n) = \cos(t) \cos(t/2 + \psi_n)$, where we neglect the detuning inside the cosine because it leads to a term of higher order in ϵ . When inserted into the right-hand side of Eq. (2.6), these terms get multiplied by $\cos(t/2 + \psi_n)$, giving only one term which does not average to zero, namely, $\epsilon \gamma/2 \cdot R_n \cos(2\psi_n)$.

Finally we consider the contributions coming from the nonlinear term in Q_n , αg_n . As discussed above, this term is composed of an infinite number of cubic terms, each of which can be put in the form $\cos[(\omega_i \pm \omega_j \pm \omega_k)t + \psi_i \pm \psi_j \pm \psi_k]$, and where i, j, k can take on any integer values. The contribution of each such term to Eq. (2.6) involves multiplying by $\cos(\omega_n t + \psi_n)$, which gives terms of the form $\cos[(\omega_i \pm \omega_j \pm \omega_k \pm \omega_n)t + \psi_i \pm \psi_j \pm \psi_k \pm \psi_n]$. Now since $\omega_n^2 = \delta + n^2 c^2$, the set of ω_n 's may be assumed to be mutually incommensurate, i.e., no resonance relation exists between any of them, e.g., $\omega_1 \neq 2\omega_0$, etc. Then, in order for the average of such a term to be nonzero, the argument inside the cosine must be zero. The only way that can happen is if the terms cancel each other, e.g., if $j=i$ and $k=n$ and the term takes the form $\cos[(\omega_i - \omega_i + \omega_n - \omega_n)t + \psi_i - \psi_i + \psi_n - \psi_n] = \cos 0 = 1$. Such a term would have come from the cubic $f_i^2 f_n$. If such a term appeared in g_n with the coefficient k , i.e., $g_n = k f_i^2 f_n + \dots$, then its contribution to the right-hand side of (2.6) would be

$$-2\epsilon \alpha k R_i^2 \cos^2(\omega_i t + \psi_i) R_n \cos^2(\omega_n t + \psi_n). \quad (\text{B9})$$

The contribution of this term to the averaged version of Eq. (2.6) would be $-\epsilon \alpha k R_i^2 R_n/2$, except if $i=n$, in which case it would be $-3\epsilon \alpha k R_n^3/4$. There will be an infinite number of such terms for a given value of n , one term for each integer i . However, we have already shown that the amplitudes R_i of all the nonresonant modes decay to zero. So we may omit such terms from the averaged equation on ψ_n , thereby restricting attention to the long-time behavior, i.e., after the transients associated with the decay of the nonresonant

modes die out. Thus the only term which contributes to the averaged equation corresponds to the case $i=n$ and has contribution $-3\epsilon\alpha k R_n^3/4$. Here k is the coefficient of the f_n^3 term in g_n . The value of k may be stated as follows: If we take just one mode for u (the other nonresonant modes decaying to zero), $u=f_n \cos nx$, then k is the coefficient of $\cos nx$ in the nonlinear term $\cos^3 nx$. If $n=0$, then $k=1$. Otherwise, the identity

$$\cos^3 x = \frac{3}{4} \cos x + \frac{1}{4} \cos 3x \quad (\text{B10})$$

shows $k=3/4$. Thus we conclude that the contribution of the αg_n term to the averaged version of Eq. (2.11) is $-9\epsilon\alpha R_n^3/16$ for $n>0$, and $-3\epsilon\alpha R_0^3/4$ for $n=0$.

Collecting all the preceding results together, we obtain the averaged equations

$$\dot{\psi}_n = \epsilon\Delta + \epsilon \frac{\gamma}{2} \cos 2\psi_n - \frac{9}{16} \epsilon\alpha R_n^2, n>0, \quad (\text{B11})$$

$$\dot{\psi}_0 = \epsilon\Delta + \epsilon \frac{\gamma}{2} \cos 2\psi_0 - \frac{3}{4} \epsilon\alpha R_0^2, n=0. \quad (\text{B12})$$

- ¹B. Denardo, "Observations of Nonpropagating Oscillatory Solitons," Ph.D. thesis, Department of Physics, University of California, Los Angeles, California, 1990.
- ²B. Denardo, W. Wright, and S. Putterman, "Observation of a kink soliton on the surface of a liquid," *Phys. Rev. Lett.* **64**, 1518–1521 (1990).
- ³B. Denardo, B. Galvin, A. Greenfield, A. Larraza, S. Putterman, and W. Wright, "Observations of localized structures in nonlinear lattices: Domain walls and kinks," *Phys. Rev. Lett.* **68**, 1730–1733 (1992).
- ⁴B. Denardo, A. Larraza, S. Putterman, and P. Roberts, "Nonlinear theory of localizing standing waves," *Phys. Rev. Lett.* **69**, 597–600 (1992).
- ⁵S. J. Putterman and P. H. Roberts, "Nonlinear theory of modulated standing waves: Domain walls, kinks, and breathers," *Proc. R. Soc. London, Ser. A* **440**, 135–148 (1993).
- ⁶B. Denardo and W. Wright, "Structural properties of kinks and domain walls in nonlinear oscillatory lattices," *Phys. Rev. E* **52**, 1094–1104 (1995).
- ⁷R. Keolian, "Modulations of Driven Nonlinear Standing Surface Waves on Water and Liquid Helium-4," Ph.D. dissertation, Department of Physics, University of California, Los Angeles, California, 1985.
- ⁸G. B. Whitham, *Linear and Nonlinear Waves* (Wiley, New York, 1974).
- ⁹R. K. Dodd, J. C. Eilbeck, J. D. Gibbon, and H. C. Morris, *Solitons and Nonlinear Wave Equations* (Academic, London, 1982).
- ¹⁰G. Eilenberger, *Solitons* (Springer, Berlin, 1983).
- ¹¹G. I. Lamb, Jr., *Elements of Soliton Theory* (Wiley, New York, 1980).

- ¹²P. G. Drazin and R. S. Johnson, *Solitons: An Introduction* (Cambridge University Press, Cambridge, 1989).
- ¹³A. R. Bishop, R. Flesch, M. G. Forest, D. W. McLaughlin, and E. A. Overman, "Correlations between chaos in a perturbed sine-gordon equation and a truncated model system," *SIAM (Soc. Ind. Appl. Math.) J. Math. Anal.* **21**, 1511–1536 (1990).
- ¹⁴A. R. Bishop, M. G. Forest, D. W. McLaughlin, and E. A. Overman, "A model representation of chaotic attractors for the driven, damped pendulum chain," *Phys. Lett. A* **144**, 17–25 (1990).
- ¹⁵N. M. Ercolani, M. G. Forest, D. W. McLaughlin, and A. Sinha, "Strongly nonlinear modal equations for nearly integrable PDEs," *J. Nonlinear Sci.* **3**, 393–426 (1993).
- ¹⁶R. Grauer and Y. S. Kivshar, "Chaotic and phase-locked breather dynamics in the damped and parametrically driven sine-gordon equation," *Phys. Rev. E* **48**, 4791–4800 (1993).
- ¹⁷J. J. Stoker, *Nonlinear Vibrations in Mechanical and Electrical Systems* (Wiley, New York, 1950).
- ¹⁸A. H. Nayfeh and D. T. Mook, *Nonlinear Oscillations* (Wiley, New York, 1979).
- ¹⁹C. A. Holmes and R. H. Rand, "Coupled oscillators as a model for nonlinear parametric excitation," *Mech. Res. Commun.* **8**, 263–268 (1981).
- ²⁰L. A. Month and R. H. Rand, "Bifurcation of 4:1 subharmonics in the nonlinear Mathieu equation," *Mech. Res. Commun.* **9**, 233–240 (1982).
- ²¹J. C. Strikwerda, *Finite Difference Schemes and Partial Differential Equations* (Wadsworth & Brooks/Cole, Pacific Grove, 1989).
- ²²R. Peyre and T. D. Taylor, *Computational Methods for Fluid Flow* (Springer, New York, 1983).
- ²³C. A. J. Fletcher, *Computational Galerkin Methods* (Springer, New York, 1984).
- ²⁴L. F. Shampine, *Numerical Solution of Ordinary Differential Equations* (Chapman & Hall, New York, 1994).
- ²⁵D. J. Jones, J. C. South, and E. B. Klunker, "On the numerical solution of elliptic partial differential equations by the method of lines," *J. Comput. Phys.* **9**, 496–527 (1972).
- ²⁶M. Holt, *Numerical Methods in Fluid Dynamics*, 2nd revised ed. (Springer, Berlin, 1984).
- ²⁷W. E. Schiesser, *The Numerical Method of Lines Integration of Partial Differential Equations* (Academic, San Diego, 1991).
- ²⁸C. S. Hsu, *Cell-to-Cell Mapping* (Springer, New York, 1987).
- ²⁹R. H. Rand, "Dynamics of a nonlinear parametrically-excited PDE: 2-term truncation," *Mech. Res. Commun.* **23**, 283–289 (1996).
- ³⁰C. Baesens, J. Guckenheimer, S. Kim, and R. S. MacKay, "Three coupled oscillators: Mode locking, global bifurcations and toroidal chaos," *Physica D* **49**, 387–475 (1991).
- ³¹R. H. Rand, W. I. Newman, B. C. Denardo, and A. L. Newman, "Dynamics of a nonlinear parametrically-excited partial differential equation," in Proceedings of the 1995 Design Engineering Technical Conferences, Vol. 3, Part A, "Vibration of nonlinear, random and time-varying systems," Boston, Massachusetts, September 17–20, 1995, A.S.M.E., **DE-84-1**, 57–68 (1995).